

Accommodation-based liquid crystal adaptive optics system for large ocular aberration correction

Quanquan Mu,^{1,2} Zhaoliang Cao,^{1,2} Chao Li,^{1,2} Baoguang Jiang,^{1,2} Lifa Hu,¹ and Li Xuan^{1,*}

¹State Key Laboratory of Applied Optics, Changchun Institute of Optics, Fine Mechanics and Physics, Chinese Academy of Sciences, Changchun, Jilin, 130033, China

²Graduate School of the Chinese Academy of Sciences, Beijing, 100039, China

*Corresponding author: xuanli@ciomp.ac.cn

Received September 2, 2008; revised October 15, 2008; accepted October 29, 2008; posted November 7, 2008 (Doc. ID 100885); published December 4, 2008

According to ocular aberration property and liquid crystal (LC) corrector characteristics, we calculated the minimum pixel demand of the LC corrector used for compensating large ocular aberrations. Then, an accommodation based optical configuration was introduced to reduce the demand. Based on this an adaptive optics (AO) retinal imaging system was built. Subjects with different defocus and astigmatism were tested to prove this. For myopia lower than 5D it performs well. When myopia is as large as 8D the accommodation error increased to nearly 3D, which requires the LC corrector to have 667×667 pixels to get a well-corrected image. © 2008 Optical Society of America

OCIS codes: 170.3890, 230.3720, 010.1080, .

Fundus imaging is one of the most important techniques for detecting and diagnosing human diseases that influence the retina. The basic instruments usually used include a fundus camera, optical coherence tomography (OCT), and a scanning laser ophthalmoscope (SLO). They have nearly $10 \mu\text{m}$ resolution owing to the aberrations of the eye. Although spectacles have been used to correct defocus [1] and astigmatism [2], they still leave uncorrected aberrations such as spherical aberration, coma, and a host of irregular aberrations, e.g., a blurred fundus image. For larger pupil diameters this degradation became even worse.

In 1961, Smirnov first suggest improving the optical performance of the eye by compensating for its aberrations [3]. In 1994, Liang *et al.* introduced the Shack–Hartmann wavefront sensor (SH sensor) for measuring the eye's aberration [4]. Based on this, a high-resolution retinal imaging adaptive optics (AO) system was built [5]. The AO technique has found a home in vision science, where it is used to further our understanding of the human retina [6].

Most AO retina imaging systems only correct high-order aberrations. Usually, trial lenses [7] and a four mirror subsystem [8] were used to correct defocus and astigmatism. The drawback is the necessity of maintaining accurately the distance between the eye and this instrument, because variation of this distance will have an influence on the aberrations. The approach is also restricted to a small field of view (FOV), since an intermediate image will tend to be rather large with an increasing FOV. If we want to compensate all the aberrations by the AO system, a large correction depth for low-order aberrations and enough spatial resolution for high-order aberrations will be needed. Consider that for a conventional deformable mirror (DM) to achieve a high precision correction it should also have at least $4N-2$ (N represents the Zernike polynomial order) actuators positioned outside the correction area for a continuous facesheet DM and $2N+1$ for bimorph and membrane DMs, resulting in a larger physical size and

more actuators [9]. It is hard and expensive to manufacture a DM that meets all these demands. Chen [10] has reported a high-resolution AO–SLO with dual DMs. A bimorph mirror and a microelectromachined systems DM were used to correct low- and high-order aberrations, respectively. Based on this, nearly $\pm 3\text{D}$ large aberrations can be well corrected, and it effectively eliminates accurate refractive error fitting of the patients, which is crucial in clinical settings. However, patients with a very large refractive error may still need a coarse adjustment using a trial lens or optometer [10]. The compensation is still limited, and the whole system is very expensive and complex.

A liquid crystal (LC) corrector is more suitable for this. It usually has millions of pixels, which makes it possible to use a phase-wrapping technique to increase the correction depth without any loss of spatial resolution. Previous work has proved its availability for large aberration compensation with small pupils [11].

In this Letter, we discuss the capability of a LC on silicon (LCOS) corrector used for compensating large eye aberrations under large pupils. According to ocular aberration properties and LCOS corrector characteristics, we calculated the minimum pixel demand for large aberration corrections. Then, an accommodation-based optical configuration was introduced to reduce the demand. Based on this, a high-resolution AO retina imaging system was built. Subjects with different low-order aberrations were tested. For myopia lower than 5D, it performs well. When myopia is as large as 8D the accommodation error increased to nearly 3D, which requires the LCOS corrector to have 667×667 pixels to get a well-corrected image.

A previous study found that low-order aberrations were the dominant aberrations of the eye. They contribute over 86% of the wavefront error (WFE) in root mean square (RMS) for a 7 mm pupil [12]. Miller [13] confirmed that for a 6 mm pupil the LC corrector

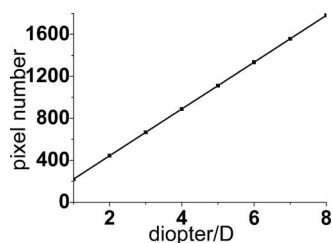


Fig. 1. Minimum pixel requirement for different diopters.

with 72×72 pixels can only handle 1D defocus, where it just reaches a Strehl of 0.8 corresponding to 0.07λ WFE in RMS. From his simulation the pixel number is linearly related with dioptr for a 0.8 Strehl ratio, which indicates that nearly 600×600 pixels could correct diopters up to 8D [13]. According to this, the edge quantified level is no more than 3, and the diffraction efficiency is as low as 68%, which will impact the detection accuracy for closed-loop applications. Our previous research has realized that the quantified level must larger than 10 to maintain nearly 85% diffraction efficiency and a continuous wavefront profile, concerning the pixel mismatch and black matrix [14,15]. For the eye, the quantified level will mostly rest with low-order aberrations. So, we use a spherical wave model to evaluate the quantified level for different diopters. The radius of the spherical wave is defined as $r = 1000/D$ (mm), where D represent dioptr.

The wavefront profile along the pupil radius d can be expressed as

$$\phi(x, D) = 1000/D - [(1000/D)^2 - x^2]^{1/2}, \quad (1)$$

where $-d \leq x \leq d$ is an arbitrary point along the pupil radius. It has the largest gradations at the pupil edge. We only need to check whether it reaches ten quantified levels at the pupil edge. For a 6 mm pupil, it can be expressed as

$$\phi(3, D) - \phi(x_1, D) = 0.1 \times \lambda. \quad (2)$$

The pixel number along the pupil diameter can be calculated by

$$N(D) = 6/(3 - x_1), \quad (3)$$

where $(3 - x_1)$ represents the maximum pixel pitch at the edge.

According to this the minimum pixel demand for myopia 1D to 8D for a 6 mm pupil is shown in Fig. 1. It indicates that with the LC corrector that has over 1781×1781 pixels we can correct over 8D diopters without any trial lens compensation, theoretically. To

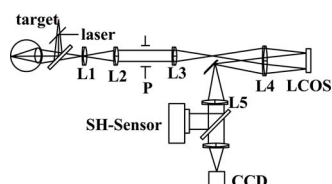


Fig. 2. (Color online) Optical layout of the retinal imaging system.

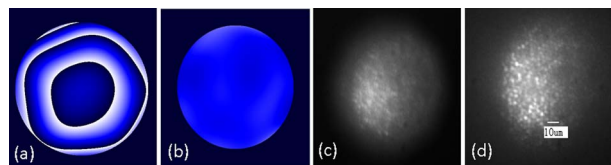


Fig. 3. (Color online) WFE and retina image of CL (a),(c) before and (b),(d) after correction.

reduce the pixel requirement and extend the correction capacity, we optimized the AO system.

A conventional AO system uses an infinite object to stabilize the eye at a relaxed condition. We know that the eye can accommodate to a finite distance target, which means automatic correction of myopia. It induced the reduction of aberration, which could reduce the demand on pixels for the LC corrector. For a different dioptr D , this finite distance equals to $1/D$ m. Under this adjustment, we can correct over 8D diopters theoretically without too many increases on the WFE.

Figure 2 shows the layout of the AO retinal imaging system. An 808 nm laser was used for illumination. A cross line target positioned 200 mm before the eye was used for stabilization. When a subject focuses on it, light reflected from the fundus will be concentrated at the same distance before the eye. Such a configuration ensures the detected defocus remains zero for subjects with myopia up to 5D. Conjugating lens pairs L1–L2, L3–L4, and L4–L5 conjugated the eye pupil with the P , the LCOS plane, and the SH sensor, respectively. The LCOS corrector manufactured by BNS Corporation has a 7.68×7.68 mm active area and 512×512 pixels with a 2π phase modulation depth. The frame rate is 200 Hz.

Three subjects with natural pupils and with different myopia and astigmatism were measured in a laboratory. Room lights were dimmed to maintain an approximately 6 mm pupil diameter. The corresponding area of the LCOS corrector was 6.6 mm in diameter with 440×440 pixels.

First, subject CL with 5D myopia was tested. The target distance was set to 200 mm. The average WFE in nearly 10 s in peak–valley (PV) before and after correction was 1.9 and $0.06 \mu\text{m}$, as shown in Figs. 3(a) and 3(b), respectively. The fundus image after correction shown in Fig. 3(d) reached the diffraction limited resolution. It proves that the accommodation-based technique reduced the WFE to nearly $0.4D$. Then, subject MX with 3D defocus and 2D astigmatism was tested. Because the accommodation can only reduce the defocus WFE, the observed WFE was $6 \mu\text{m}$ in PV, which is mainly the astigmatism and in the range of LCOS correction capability. The correction precision was $0.12 \mu\text{m}$ in PV shown in Fig. 4(b).

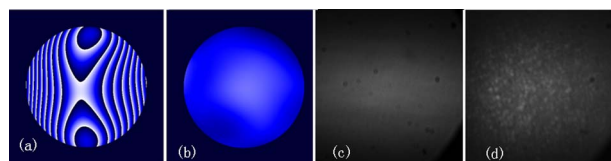


Fig. 4. (Color online) WFE and retina image of MX (a),(c) before and (b),(d) after correction.

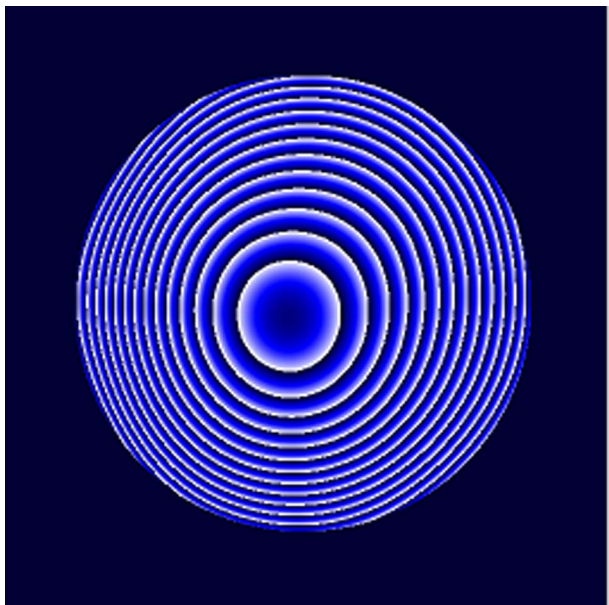


Fig. 5. (Color online) WFE for subject ZP with 8D myopia. The fundus image was shown in Figs. 4(c) and 4(d).

Then, the target was set to 125 mm before the eye pupil to match the subject ZP who has 8D myopia. All the components at the left of lens L2 were moved together at the same time to change the distance between lens L1 and L2 to ensure the parallel light output. The subject was asked to focus on the cross line target until a clear observation was reached. But the detected WFE still remains $10.2 \mu\text{m}$, as shown in Fig. 5, which is nearly 2.3D and exceeds the correction possibility.

This was not what was anticipated. We consider that it is related to the accommodation error. It has been reported that observers failed to accommodate “accurately” both at low and high dioptric stimulus levels. The increased errors in focus for near targets were evident and the exact value of the accommodative lag showed a significant intersubject variability [16]. According to the detected WFE the accommodation error for ZP and CL are 2.27D and 0.4D, respectively, which is congruous (in the fluctuation range) with [16].

In summary, we calculated the minimum pixel demand for high amplitude WFE correction. An accommodation-based technique was introduced to reduce the pixel requirement and extend the correc-

tion capacity. The experiment proves that it is feasible. It has the best performance for myopia of no more than 5D. The deviation due to the accommodation error increases linearly with the target vergence. The maximum accommodation error for the 8D is nearly 3D. So, the pixel demand for the LC corrector can be reduced from 1781×1781 to 667×667 for a good correction of 8D diopters. However, this accommodation-based technique can correct only myopia. For a large astigmatism, which exceeds the dynamic range of the LC corrector, a spectacle compensator may be needed and can be inserted in position *P* in Fig. 2.

This work is supported by the National Natural Science Foundation of China (NSFC) (60578035, 50473040, 60736042, and 60811120025) and the Science Foundation of Jilin Province (20050520, 20050321-2).

References

1. M. L. Rubin, *Surv. Ophthalmol.* **30**, 321 (1986).
2. H. von Helmholtz, *Helmholtz's Treatise on Physiological Optics*, J. P. C. Southall, ed. (Optical Society of America, 1924).
3. M. S. Smirnov, *Biophysics (Engl. Transl.)* **6**, 766 (1961).
4. J. Liang, B. Grimm, S. Goelz, and J. Bille, *J. Opt. Soc. Am. A* **11**, 1949 (1994).
5. J. Liang, D. R. Williams, and D. T. Miller, *J. Opt. Soc. Am. A* **14**, 2884 (1997).
6. J. Carroll, D. C. Gray, A. Roorda, and D. R. Williams, *Opt. Photon. News* **16**, 36 (2005).
7. J. Rha, R. S. Jonnal, K. E. Thorn, J. Qu, Y. Zhang, and D. T. Miller, *Opt. Express* **14**, 4552 (2006).
8. E. J. Fernandez, I. Iglesias, and P. Artal, *Opt. Lett.* **26**, 746 (2001).
9. G. Vdovin, O. Soloviev, A. Samokhin, and M. Loktev, *Opt. Express* **16**, 2859 (2008).
10. D. C. Chen, S. M. Jones, D. A. Silva, and S. S. Olivier, *Proc. SPIE* **6426**, 64261L1 (2007).
11. Q. Mu, Z. Cao, D. Li, L. Hu, and L. Xuan, *Opt. Express* **15**, 1946 (2007).
12. J. F. C. Mochon, N. L. Gil, A. Benito, and P. Artal, *Vision Res.* **42**, 1611 (2002).
13. D. T. Miller, L. N. Thibos, and X. Hong, *Opt. Express* **13**, 275 (2005).
14. Z. Cao, Q. Mu, L. Hu, Y. Liu, and L. Xuan, *Chin. Phys.* **16**, 1665 (2007).
15. Z. Cao, L. Xuan, L. Hu, Y. Liu, and Q. Mu, *Opt. Express* **13**, 5186 (2005).
16. S. Plainis and H. S. Ginis, *J. Vision* **5**, 466 (2005).